Adiponectin overexpression improves metabolic abnormalities caused by acid ceramidase deficiency but does not prolong lifespan in a mouse model of Farber Disease

Marie K. Norris [a,b], Trevor S. Tippetts [a,b,c], Joseph L. Wilkerson [a,b], Rebekah J. Nicholson [a,b], J. Alan Maschek [d], Thierry Levade [e], Jeffrey A. Medin [f], Scott A. Summers [a,b], William L. Holland [a,b,*]

[a] Department of Nutrition and Integrative Physiology, University of Utah College of Health, Salt Lake City, UT, USA
[b] Diabetes and Metabolism Research Center, University of Utah College of Medicine, Salt Lake City, UT, USA
[c] Children's Research Institute, University of Texas Southwestern Medical Center, Dallas, TX, USA
[d] Metabolomics Core Facility, University of Utah, Salt Lake City, UT, USA
[e] Laboratoire de Biochimie Métabolique, CHU Toulouse and INSERM U1037, Centre de Recherches en Cancérologie de Toulouse, Université Paul Sabatier, 31037 Toulouse, France
[f] Departments of Pediatrics and Biochemistry, Medical College of Wisconsin, Milwaukee, WI, USA

ARTICLE INFO

ABSTRACT

Farber Disease is a debilitating and lethal childhood disease of ceramide accumulation caused by acid ceramidase deficiency. The potent induction of a ligand-gated neutral ceramidase activity promoted by adiponectin may provide sufficient lowering of ceramides to allow for the treatment of Farber Disease. In vitro, adiponectin or adiponectin receptor agonist treatments lowered total ceramide concentrations in human fibroblasts from a patient with Farber Disease. However, adiponectin overexpression in a Farber Disease mouse model did not improve lifespan or immune infiltration. Intriguingly, mice heterozygous for the Farber Disease mutation were more prone to glucose intolerance and insulin resistance when fed a high-fat diet, and adiponectin over-expression protected from these metabolic perturbations. These studies suggest that adiponectin evokes a ceramidase activity that is not reliant on the functional expression of acid ceramidase, but indicates that additional strategies are required to ameliorate outcomes of Farber Disease.

1. Introduction

Farber Disease (OMIM #228000), first described by Sidney Farber in 1952, is one of nine described lysosomal storage diseases leading to aberrant accumulation of sphingolipids [1]. Caused by biallelic mutations in the lysosomal *ASAH1* gene, patients with Farber Disease have an impaired capacity to degrade ceramide within the lysosome [1–4]. The resulting deficiency leads to the overaccumulation of ceramides in the lysosome and other cellular compartments [1,5]. Increased ceramides lead to lipotoxicity and apoptotic death of numerous cell types. Compared to being diagnosed through state newborn screening, patients with Farber Disease are diagnosed symptomatically and present with three main symptoms: lipogranulomas, contractures, and hoarseness of voice [5]. Although there is a spectrum in disease presentation (Farber Disease Type 1–5), additional symptoms of the classic form include brain atrophy, progressive cognitive and motor impairments, anemia, leukocytosis, thrombocytosis, liver failure, and significant lipid deposition in the heart and alveoli [5]. Cardiac and pulmonary functions decline and are often the ultimate cause of childhood mortality in the classic form of this invariably fatal disease [3,5]. Although Farber Disease is extremely rare with <100 cases described in medical literature, the actual number of cases is likely underestimated due to misdiagnosis

[4].

While Farber disease is the most common form of an *ASAH1* gene alteration, there is a unique form of *ASAH1*-related disorders with an almost exclusive neurological pathology and is characterized by degeneration of motor neurons in the spinal cord leading to muscle atrophy and seizures called spinal muscular atrophy with progressive myoclonic epilepsy (SMA-PME) [6]. Due to different mutations in the *ASAH1* gene from the Farber Disease mutations, patients with SMA-PME present with motor deficits around age 3 and progress to muscle paralysis with myoclonic epilepsy refractory to conventional therapy and death due to respiratory muscle degeneration before 20 years of age [6]. Recently, a mouse model of SMA-PME was developed with progressive neurological deterioration of the spinal cord and could aid in studying the distinct and complex pathologies caused by *ASAH1*-related disorders [7].

With limited treatment options, there remains an urgent need for novel therapeutics to treat Farber Disease. Currently, palliative care and treating individual symptoms are the only options for patients with Farber Disease [5]. Enzyme replacement therapy has gained traction for several lysosomal storage diseases, including Farber Disease [8,9]. However, these soluble enzymes cannot cross the blood-brain barrier, thus limiting efficacy against the neurodegenerative effects of these diseases, and this option still has yet to gain FDA approval for treatment [8].

Patients with Farber Disease have a deficiency in acid ceramidase, which degrades ceramides into sphingosine and a fatty acid [10]. De novo ceramide synthesis begins with the condensation of palmitoyl-CoA and serine to produce 3-ketosphinganine via serine palmitoyl transferase (SPT) [11]. 3-Ketosphinganine is quickly reduced to sphinganine by 3-ketosphinanine reductase. Various length fatty acid chains are added to the sphinganine backbone catalyzed by one of the (dihydro) ceramide synthases (CERS1–6) to form dihydroceramide [11]. A 4,5-trans double bond is added to the sphingoid backbone by dihydroceramide desaturase 1 (DES1) to form ceramide [11]. The addition of this double bond changes the molecule's biological activity into a lipotoxic signaling molecule by modifying its elastic properties and packing behavior [12].

Over the last 30 years, a growing consensus agrees that ceramides are universal signals of cellular stress that modulate metabolism and induce apoptosis [11,13]. During prolonged nutrient overload, accumulation of lipotoxic ceramides contributes to cardiovascular disease, type 2 diabetes, and non-alcoholic steatohepatitis (NASH) by decreasing insulin signaling, increasing triglyceride storage, and decreasing mitochondrial performance [13,14]. Remarkably, inhibition of ceramide biosynthesis in rodents ameliorates many conditions including cystic fibrosis, asthma, NASH, type 2 diabetes, heart failure, and chronic kidney disease [15–44]. Owing to a strong association of serum ceramides with cardiovascular disease and all-cause mortality [45–56], the Mayo Clinic is now marketing tests to measure circulating ceramides as markers of disease risk [57,58]. Because of these findings, ceramide synthesis inhibitors are being explored as novel therapeutics.

Adiponectin is a hormone released by adipocytes and found to have beneficial effects on insulin sensitivity, inflammation, and survival [33]. Once released, adiponectin binds to either adiponectin receptor 1 (AdopoR1) or adiponectin receptor 2 (AdipoR2) to initiate this broad spectrum of cellular actions [33,59]. AdipoR1 and AdipoR2 are involved in the transcriptional regulation of genes to decrease inflammation, decrease senescence, decrease apoptosis and oxidative stress, and increase nitric oxide production [59]. Mice lacking these receptors show metabolic dysfunction, including insulin resistance and hyperglycemia [60]. Furthermore, we recently demonstrated that adiponectin increases ceramide breakdown when bound to AdipoR1/AdipoR2 receptors [33]. AdipoR1 and AdipoR2 contain innate ceramidase activity, which degrades ceramides and improves insulin sensitivity in mice after administration of recombinant adiponectin [33]. We hypothesized that lowering ceramides with adiponectin administration can improve outcomes in Farber Disease patients.

We studied mice with a missense mutation in *ASAH1* (ASAH1$^{P361R/P361R}$) that is analogous to a mutation identified in Farber Disease patients (NM_177924.5(*ASAH1*):c.1085C > G (p.Pro362Arg)) [61]. These mice reach maximum weight at 5 weeks, exhibit progressive growth retardation, accumulate inflammatory markers in tissues, show ceramide accumulation in blood, tissues, and skin, have a near complete loss of hypodermal adipose tissue, have stiff neck skin, and display sex-specific pathologies (e.g., small ovaries or penile prolapse) [61,62]. Further, these mice only survive between 7 and 13 weeks [61]. A previous study identified that a truncated adiponectin protein lacking a portion of the collagenous domain (ΔGly^{Tg}) increased whole-body expression of adiponectin 3-fold compared to full-length adiponectin [63]. We crossed these two mouse models to generate whole-body adiponectin overexpression in the Farber Disease model (ASAH1$^{P361R/P361R}$ΔGly^{Tg}). The findings confirmed that adiponectin overexression was sufficient to improve the metabolic health of heterozygous animals. However, it could not reverse homozygous acid ceramidase deficiency's more severe pathogenic features.

2. Materials and methods

2.1. Farber Disease fibroblasts

We obtained Farber Disease patient fibroblasts [64,65] from Thierry Levade. Fibroblasts (passage number < 10) were cultured in standard Dulbecco's Modified Eagle's Medium (Gibco™; 11965118) supplemented with 10% fetal bovine serum (ATCC®; 30–2020) and 1% penicillin/streptomycin (ATCC®; 30–2300). Fibroblasts were seeded equally with 1×10^6 cells per well. Fibroblasts were treated with 0.3 μg/ml (10.4 nM) of Adiponectin, 25 μM of AdipoRon, or a PBS control. Ceramide measurements were completed 24 h after stimulation. Ceramide content was normalized relative to PBS-control-treated fibroblasts. Cell viability (>95% by trypan blue exclusion) assay was not affected by treatment conditions.

2.2. Mice

All animal procedures complied with protocols approved by the Institutional Animal Care and Use Committee (IACUC) at the University of Utah. Mice were housed in groups of 2–5 at 22 °C–24 °C using a 12-h light/12-h dark cycle with ad libitum access to water at all times. Mice were fed a chow diet (13% fat, 58% carbohydrate, 29% protein, Bio-Serv), or high-fat diet (HFD) (60% fat, 26% carbohydrate, 15% protein, Bio-Serv) from the age of 8 weeks as indicated.

2.3. Generation of ASAH1$^{P361R/P361R}$ΔGly^{Tg} mice

We obtained ASAH1$^{P361R/P361R}$ mice on a mixed background from Jeffrey Medin, who originally generated and characterized the mice [61]. Additionally, we obtained ΔGly^{Tg} mice [63] on a C57Bl6 background from Philipp Scherer. Using these mice, we generated a novel transgenic mouse line (ASAH1$^{P361R/P361R}$ΔGly^{Tg}) allowing for whole-body transgenic over-expression of adiponectin in the Farber Disease model. We backcrossed the mice >3 generations to C57Bl6 background. Mice without the ΔGly transgene were used as controls for mice containing wild-type, heterozygous, and homozygous mutations for the human Farber Disease mutation. We also overexpressed an inducible form of the adiponectin receptor, AdipoR2, by crossing a (Tet-on) TRE-AdipoR2 transgenic mice [66] under the control of cytomegalovirus-driven rtTA (Jackson Labs strain #003273).

Gene	Validated PCR Primer Sets
ASAH1 P361R Mut	(F) 5′-GCTGGACGTAAACTCCTCTTCAGACC-3′
	(R) 5′-TCAAGGCTTGACTTTGGGGCAC-3

(continued on next page)

(*continued*)

Gene	Validated PCR Primer Sets
ASAH1 P361R WT	(F) 5′-CAGAAGGTATGCGGCATCGTCATAC-3′
	(R) 5′-AGGGCCATACAGAGAGAAACCCTGTCTC-3
ΔGly	(F) 5′-GTTCCTCTTAATCCTGCCCATC-3′
	(R) 5′CCCGGAATGTTGCAGTAGAACTTG-3′
Cytomegalovirus rtTA	(F) 5′-CGCTGTGGGGCATTTTACTTTAG-3′
	(R) 5′-CATGTCCAGATCGAAATCGTC-3′
TRE-AdipoR2	(F) 5′-TGTGACATCTGGTTTCACTCTC-3′
	(R) 5′-TGGTGATACAAGGGACATCTTC-3′

2.4. Western Blot analysis

Plasma was mixed with protease inhibitors (Halt™), sample buffer (Bolt™), and reducing agent (Bolt™). 10 µl of plasma was resolved using precast Bolt (4–12% Bis-Tris gels, Invitrogen) and transferred to Nitrocellulose membranes (GE Healthcare). Membranes were blocked with 5% BSA in Tris-buffered saline containing 0.05% Tween-20 (TBST) and incubated with primary antibodies (anti-adiponectin Abcam; ab22554) at 4 °C overnight with subsequent 1-h incubation with secondary fluorescent antibodies (Invitrogen; A32729) and normalized to total protein (Ponceau).

2.5. Analytical procedures

Blood glucose levels were determined from whole blood using an automatic glucose monitor (Bayer Contour, Bayer, Germany). Insulin levels in serum were measured by CrystalChem mouse ultra sensitive insulin ELISA assay using mouse standards according to the manufacturer's guidelines (CrystalChem, USA, 90080).

2.6. Myriocin treatment

Myriocin was dissolved in methanol to prepare a 5 mM stock solution and diluted in PBS (0.15mM) prior to injection. Mice were injected intraperitoneally with either 0.3 mg/kg Myriocin (Sigma, M1177-5MG) or vehicle every other day beginning at 4 weeks of age until death. Mice were randomly assigned to treatment groups.

2.7. Lipidomics

LC-MS/MS-grade solvents and mobile phase modifiers were obtained from Honeywell Burdick & Jackson, Morristown, NJ (acetonitrile, isopropanol, formic acid), Fisher Scientific, Waltham, MA (methyl tert-butyl ether) and Sigma–Aldrich/Fluka, St. Louis, MO (ammonium formate, ammonium acetate). Lipid standards were obtained from Avanti Polar Lipids, Alabaster, AL.

Lipid Standard	Avanti Catalog Number
Cer(d18:1/16:0)	Avanti 860676P
Cer(d18:1/18:0)	Avanti 860677P
Cer(d18:1/24:0)	Avanti 860678P
Cer(d18:1/24:1)	Avanti 860679P

2.7.1. Sample preparation

Frozen tissues were sectioned on dry ice and added to phosphate-buffered saline (PBS; Corning) and LC-MS/MS-grade methanol (MeOH, Fisher Scientific) containing internal stable isotope metabolomics standards (Avanti Polar Lipids). Tissues were mechanically homogenized (Qiagen TissueLyser) for 5 min at the maximum frequency (30 Hz). An aliquot was removed for protein quantification (Pierce™ BCA Protein Assay Kit). Samples were extracted using a modified Matyash method with methyl tert-butyl ether (MTBE), MeOH and PBS [67]. Samples were dried in a miVac vacuum pump (SP Scientific) and then resuspended in isopropanol: acetonitrile: dd-H2O (8:2:2). Supernatant was transferred to glass vials with inserts (Agilent, 5182–0554, 5183–2086).

2.7.2. LC-MS/MS analysis

Lipid extracts were separated on an Acquity UPLC CSH C18 column (2.1 × 100 mm; 1.7 µm) coupled to an Acquity UPLC CSH C18 VanGuard precolumn (5 × 2.1 mm; 1.7 µm) (Waters, Milford, MA) maintained at 65 °C connected to an Agilent HiP 1290 Sampler, Agilent 1290 Infinity pump, and Agilent 6490 triple quadrupole (QqQ) mass spectrometer. In positive ion mode, sphingolipids are detected using dynamic multiple reaction monitoring (dMRM). Source gas temperature is set to 175 °C, with a gas (N2) flow of 15 l/min and a nebulizer pressure of 30 psi. Sheath gas temperature is 250 °C, sheath gas (N2) flow of 12 l/min, capillary voltage is 3500 V, nozzle voltage 500 V, high pressure RF 190 V and low pressure RF is 120 V. Injection volume is 3 µl and the samples are analyzed in a randomized order with the pooled QC sample injection eight times throughout the sample queue. Mobile phase A consists of ACN:H2O (60:40 *v/v*) in 10 mM ammonium formate and 0.1% formic acid, and mobile phase B consists of IPA:ACN:H2O (90:9:1 v/v/v) in 10 mM ammonium formate and 0.1% formic acid. The chromatography gradient starts at 15% mobile phase B, increases to 30% B over 0.7 min, increases to 60% B from 0.7 to 1.4 min, increases to 80% B from 1.4 to 7.0 min, and increases to 99% B from 7.0 to 7.14 min where it's held until 9.45 min then returned to starting conditions at 9.8 min. Post-time is 3.5 min and the flowrate is 0.4 ml/min throughout. Collision energies and cell accelerator voltages were optimized using sphingolipid standards with dMRM transitions as $[M + H] + \rightarrow [m/z = 284.3]$ for dihydroceramides, $[M + H] + \rightarrow [m/z = 264.2]$ for ceramides, $[M + H] + \rightarrow [m/z = 271.3]$ for isotope labeled ceramides. Sphingomyelins and phosphatidylcholines were monitored with dMRM transitions as $[M + H] + \rightarrow [m/z = 184.1]$. Glycerolipids were monitored with dMRM transitions as $[M + NH4] + \rightarrow [m/z =$ neutral loss of acyl chain$]$. Lipids without available standards were identified based on HR-LC/MS, quasi-molecular ion and characteristic product ions. Their retention times were either taken from HR-LC/MS data or inferred from the available sphingolipid standards.

2.7.3. LC-MS/MS data processing

Results from LC-MS/MS experiments were collected using Agilent Mass Hunter Workstation and analyzed using the software package Agilent Mass Hunter Quant B.07.00. Lipid species were quantified based on the ratio to species and/or class-specific internal standards. Lipidomics were performed at the Metabolomics Core Facility at the University of Utah. Mass spectrometry equipment was obtained through NCRR Shared Instrument Grant 1S10OD016232-01A1, 1S10D018210-01A1, and 1S10OD021505–01.

2.8. Quantification of ceramidase activity

Ceramidase activity was assessed as described previously [68], with modifications. Briefly, liver homogenate was incubated at 37C for 90 min with 10 nmol/sample Cer(d18:1-d7/15:0) in a 200 uL reaction containing 12.5 mM Tris base, 3.75% oxtylβ-D-glucopyranoside, 2.5 mM cardiolipin, and 0.5 mM diethylenetriaminepentaacetic acid (pH 6.5). Process blanks contained equivalent amounts of substrate without tissue homogenate. Reactions were terminated with the addition of 600ul chloroform:methanol (1:1, *v/v*) with 25 pmol/sample Cer(d18:1/17:0) and 500 pmol/sample C17 sphingosine (d17:1) internal standards. Samples were vortexed and incubated at room temperature for 5 min before centrifugation at 15000 ×*g* for 5 min. Lipids were extracted from the organic layer and evaporated to dryness using a miVac vacuum pump. Samples were resuspended in 300 µl isopropyl alcohol:acetonitrile:water (8:2:2, v/v), vortexed, and centrifuged for 5 min at 15000 ×*g*. The supernatant and pooled quality control were transferred to a glass vials and stored at −20 °C prior to LC-MS/MS analysis. Cer(d18:1/15:0)

and sphingosine-d7 (d18:1-d7) were quantified based on peak area ratio to internal standards.

Lipid Standard	Avanti Catalog Number
Cer(d18:1/17:0)	Avanti 860,517
Cer(d18:1-d7/15:0)	Avanti 810211P
C17 sphingosine (d17:1)	Avanti 860,640

LC-MS/MS Analysis. Same as above.
LC-MS/MS Data Processing. Same as above.

2.9. Quantification of RNA

Tissues were excised from mice and snap-frozen in liquid nitrogen. Total RNA was extracted from respective tissues and cells using the Direct-zol RNA MinoPrep kit (Zymo Research) according to the manufacturer's instructions. Isolated total RNA was reverse-transcribed into cDNA using commercially available kits (Quantabio). All subsequent RT-qPCR reactions were performed on a QuantStudio 12 K Flex Real-Time PCR system (Thermo Fisher Scientific) using the Qiagen Quanti-Fast SYBR Green PCR kit. On-target amplification was verified with melt curves. Threshold cycles (Ct-values) of all replicate analyses were normalized to beta-actin for mouse tissues within each sample to obtain sample-specific ΔCt values (= Ct gene of interest - Ct, Actin,). To compare the effect of various treatments with untreated controls, 2-$\Delta\Delta$Ct values were calculated to obtain fold expression levels, where $\Delta\Delta$Ct = (ΔCt treatment - ΔCt control).

Gene	Validated RT-qPCR Primer Sets
Beta-actin	(F) 5′-GATTGCTGACAGGATGCAGAAGG-3′
	(R) 5′TGCTGGAAGGTGGACAGTGAGG-3
TNF-α	(F) 5′GGTGCCTATGTCTCAGCCTCTT-3′
	(R) 5′-GCCATAGAACTGATGAGAGGGAG-3′
IL-1β	(F) 5′-TGGACCTTCCAGGATGAGGACA-3′
	(R) 5′-GTTCATCTCGGAGCCTGTAGTG-3′
IL-6	(F) 5′TACCACTTCACAAGTCGGAGGC-3′
	(R) 5′-CTGCAAGTGCATCATCGTTGTTC-3′
MCP-1	(F) 5′-GCTACAAGAGGATCACCAGCAG-3′
	(R) 5′-GTGTGGAGGCATTCCTTCTTGG-3
AdipoR1	(F) 5′- TCTGCCTCAGTTTCTCCTGGCT-3′
	(R) 5′- GTAATAGAGCCAGGGAACGAAGC-3′
AdipoR2	(F) 5′- GGTAGATGAAGCAAGGTTGTGGG-3′
	(R) 5′- TCTTCCAGACGGTGTACTGCCA-3′

2.10. Plasma immunoassays

Cytokines were measured in plasma with a custom ProcartaPlex Multiplex Panel (ThermoFisher) on a Luminex MAGPIX® system.

2.11. Histology analysis

Freshly dissected tissues were fixed in 10% buffered formalin for 24 h and then in 70% ethanol immediately preceding embedding. Fixed tissues were embedded in paraffin, sectioned at 4 μm, and stained with hematoxylin and eosin by Associated Regional and University Pathologists (ARUP) laboratories. Slides were imaged with a Zeiss Axio Scan.Z1 and quantified with ImageJ (NIH).

2.12. Metabolic tests

Glucose-tolerance tests were performed on 12-week-old mice after a 5-h fast. After the determination of basal blood glucose concentrations, glucose was injected (intraperitoneal injection of a 20% solution, 10 ml/kg body weight) and blood glucose concentrations in blood were measured after 0, 15, 30, 60, and 120 min with a glucometer. Insulin tolerance tests were performed on 13-week-old mice after 5 h of fasting. After the determination of basal blood glucose concentrations, each mouse received an intraperitoneal injection of insulin (0.75 IU per kg body weight; Novolin; Novo Nordisk), and glucose concentrations in blood were measured after - 0, 10, 20, 30 and 60 min. Pyruvate tolerance tests were performed on 14-week-old mice after 5 h of fasting. The pyruvate solution was verified to have a neutral pH. After the determination of basal blood glucose concentrations, pyruvate was injected (intraperitoneal injection of a 10% solution, 10 ml/kg body weight) and glucose concentrations in blood were measured after 0, 15, 30, 60, and 120 min.

2.13. Hyperinsulinemic-euglycemic clamps

Insulin sensitivity was determined by a Hyperinsulinemic-euglycemic clamp. Hyperinsulinemic euglycemic clamps were performed on conscious, 5 h-fasted, unrestrained mice using an instech mouse infusion kit (Instech Labs) to allow free movement. After 9 weeks on a high-fat diet, 16-week-old mice were surgically implanted with jugular vein and carotid artery catheters and allowed to recover to their original body weight (approximately one week). On day 8, mice were fasted for ~5 h and at $t = -90$ min, after the initial blood draw, a primed continuous infusion of [U13C]glucose (~50 μmoles/ml) was started and blood samples were collected at $t = -15$ and $- 5$ min to measure basal glucose turnover. At $t = 0$ min, the clamp procedure was initiated by continuous infusion of insulin (5 mU/kg/min). Blood glucose levels were measured at 5-min intervals and maintained at euglycemia (~120 mg/dl) by a variable infusion rate of dextrose (30%) mixed with 3Hglucose (~50 μmoles/ml). Blood samples were collected during steady-state conditions ($t = 80$–120 min), every 10 min, to determine endogenous glucose appearance rate and glucose disposal rate.

2.14. Statistics

Results are provided as means ± SEM. Statistical analyses were performed using GraphPad Prism. Differences between groups were determined by one-way or two-way analysis of variance (ANOVA) with repeated measures as appropriate. For comparisons between two independent groups, a Student's *t*-test was used. Significance was accepted at $p < 0.05$.

3. Results

3.1. Adiponectin and receptor agonists deplete ceramides in fibroblasts from a patient with Farber Disease

We first evaluated whether adiponectin lowered ceramides in skin fibroblasts obtained from a patient with non-detectable acid ceramidase activity and severe Farber Disease, dying when the patient was <1 week of age [64,65]. Treating the cells with adiponectin or an adiponectin receptor agonist (AdipoRon) lowered total ceramide concentrations in cells (Fig. 1). Given this information, we decided to investigate whether genetic over-expression of adiponectin would increase lifespan and improve outcomes in a mouse model of Farber Disease.

3.2. Adiponectin overexpression does not increase lifespan in Farber Disease mice

We employed a mouse model of Farber Disease that harbors P361R point mutations in both ASAH1 alleles (ASAH1[P361R/P361R]). We crossed the ASAH1^{+/+} and ASAH1[P361R/P361R] animals with transgenic mice that overexpress an active adiponectin transgene (ΔGly[Tg]), which display several-fold increases in plasma adiponectin compared to animals lacking the construct (Fig. 2A). Adiponectin overexpression failed to influence the growth or survival phenotypes characteristic of Farber Disease in male mice (Fig. 2B-D). However, glucose concentrations trended down in ASAH1[P361R/P361R]ΔGly[Tg] males, suggesting that the adipokine increased insulin sensitivity (Fig. 2C). We observed a similar
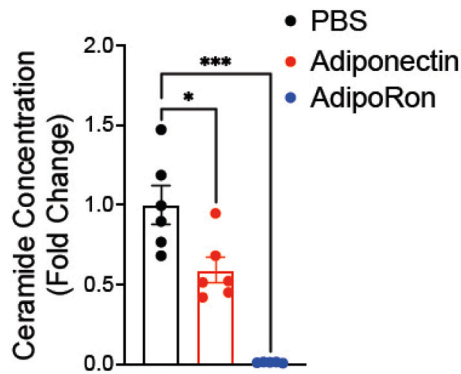
Fig. 1. Adiponectin and receptor agonists (AdiopoRon) deplete ceramides in fibroblasts from a patient with Farber Disease.
Fibroblasts were treated with 0.3 μg/ml (10.4 nM) of adiponectin, 25 μM of Adiporon, or a PBS control. Ceramide measurements were completed 24 h after stimulation. Ceramide content was normalized relative to PBS-control-treated fibroblasts. $N = 5$ technical replicates per group. Data are representative of 3 independent experiments. Individual values reported with mean ± SEM *p < 0.05, **p < 0.01, ***p < 0.001.

pattern in female mice (Appendix B).

As an alternative means of upregulating adiponectin signaling, we also overexpressed an inducible form of the adiponectin receptor, AdipoR2. At baseline, we observed decreased liver expression of AdipoR2

and increased expression of both AdipoR1 and AdipoR2 in brains and spleens of Farber Disease males (Appendix A). This is a compensatory action to degrade ceramide in the absence of acid ceramidase. This pattern was not observed in female mice; however, they showed increased brain AdipoR2 expression, demonstrating compensation by AdipoR2 (Appendix A). We found that doxycycline-inducible AdipoR2 overexpression shortened the lifespan of ASAH1$^{P361R/P361R}$ mice to five weeks (Appendix A). We hypothesize that acid ceramidase and AdipoR2 are competing ceramidases that deacylate ceramide. In the absence of acid ceramidase activity, we anticipate higher flux of ceramide through AdipoR2, which may drive greater formation of pro-inflammatory lipids, leading to a shorter lifespan. Lastly, we treated ASAH1$^{P361R/P361R}$ mice with Myriocin, a potent de novo ceramide synthesis inhibitor. Compared to vehicle-treated mice, Myriocin treatment did not increase lifespan in male ASAH1$^{P361R/P361R}$ mice (Fig. 2E).

3.3. Adiponectin overexpression lowers ceramides in plasma, but not heart, liver, spleen, or brain, of male ASAH1$^{P361R/P361R}$ mice

To determine whether adiponectin overexpression lowered ceramides in ASAH1$^{P361R/P361R}$ mice, we quantified ceramides in plasma as well as several tissues in 10-week-old mice on a normal chow diet. Overexpression of the ΔGly adiponectin transgene significantly decreased plasma ceramides in male ASAH1$^{P361R/P361R}$ mice compared to non-transgenic Farber Disease controls (Fig. 3A). By contrast, it failed to reduce ceramides in heart, liver, spleen, and brain tissue (Fig. 3B-E),
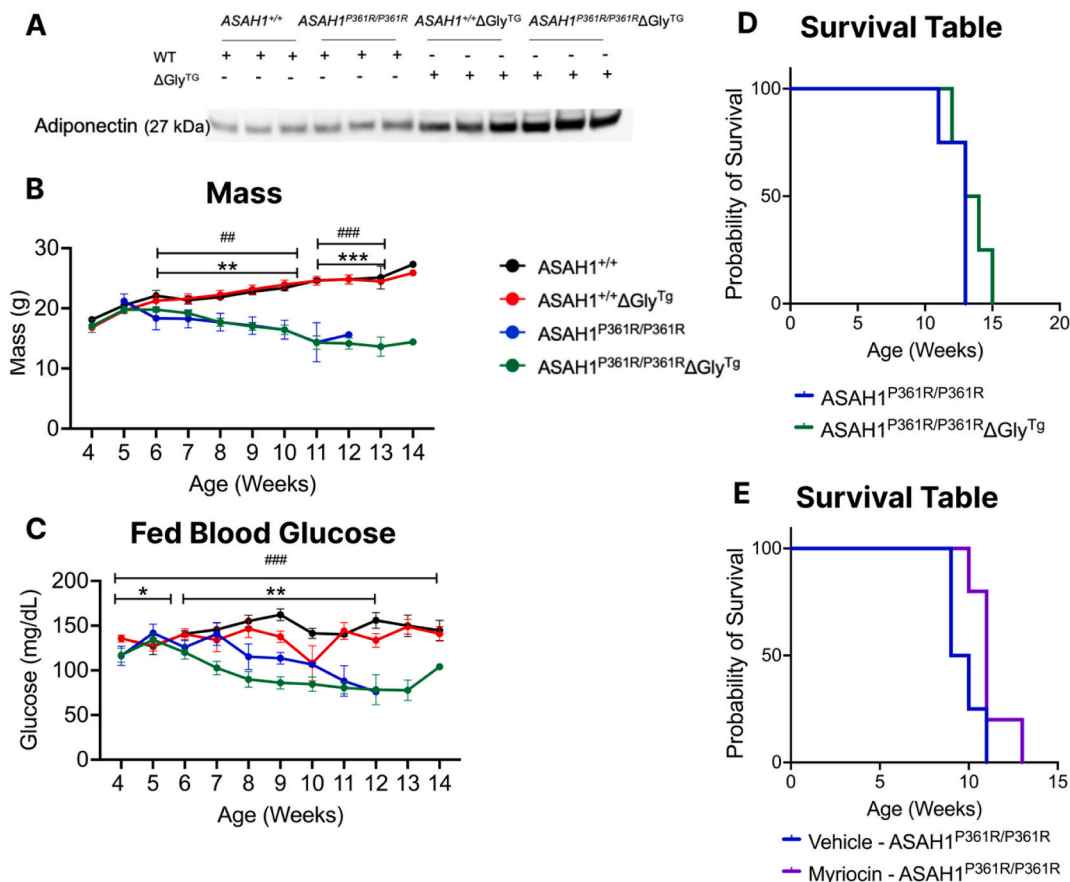

Fig. 2. Adiponectin overexpression does not increase lifespan in Farber Disease mice.
(A) Adiponectin protein immunoblot from plasma of male ASAH1$^{+/+}$ and ASAH1$^{P361R/P361R}$ mice with and without adiponectin overexpression. (B) Growth curves measured in weights versus age, *ASAH1$^{+/+}$ versus ASAH1$^{P361R/P361R}$, #ASAH1$^{+/+}$ΔGly^{Tg} versus ASAH1$^{P361R/P361R}$ΔGly^{Tg},$n = 4$–10 for each genotype, males; (C) Fed blood glucose curve, *ASAH1$^{+/+}$ versus ASAH1$^{P361R/P361R}$, #ASAH1$^{+/+}$ΔGly^{Tg} versus ASAH1$^{P361R/P361R}$ΔGly^{Tg},n = 4–10 for each genotype, males; (D) Kaplan-Meier survival analysis in Farber Disease mice with and without adiponectin overexpression, males; (E) Kaplan-Meier survival in either vehicle-treated or Myriocin-treated Farber Disease mice, males. Individual values reported with mean ± SEM *p < 0.05, **p < 0.01, ***p < 0.001.

and this was verified with a ceramidase activity assay (Fig. 3G). Adiponectin overexpression did not increase the labeled sphingosine to labeled ceramide ratio in ASAH1$^{P361R/P361R}$ΔGly^{Tg} males (Fig. 3G). In females, overexpression of the ΔGly transgene failed to impact ceramides in either plasma or tissues (Appendix C).

3.4. Adiponectin overexpression decreases pro-inflammatory cytokines in ASAH1$^{P361R/P361R}$ mice

Inflammation plays a large role in Farber Disease as patients with severe disease succumb to infections at the end of life, which is typically around two years of age in the classical manifestation [5]. A previous

study indicates widespread macrophage infiltration in tissues of ASAH1$^{P361R/P361R}$ mice as well as elevated plasma cytokines [61]. To investigate whether adiponectin overexpression reduces inflammation in ASAH1$^{P361R/P361R}$ ΔGly^{Tg} mice, we first measured the RNA expression of several pro-inflammatory cytokines including tumor necrosis factor-alpha (TNF-α), interleukin-1 beta (IL-1β), interleukin-6 (IL-6) and monocyte chemo-attractant protein-1 (MCP-1) relative to beta-actin in heart, liver, spleen and brain tissues from 10-week-old mice. As anticipated, we found elevated expression of pro-inflammatory cytokines in all four tissues from Farber Disease mice (Fig. 4A-D and Appendix D). Expression of the adiponectin transgene reduced levels of mRNA encoding pro-inflammatory cytokines in most tissues of the
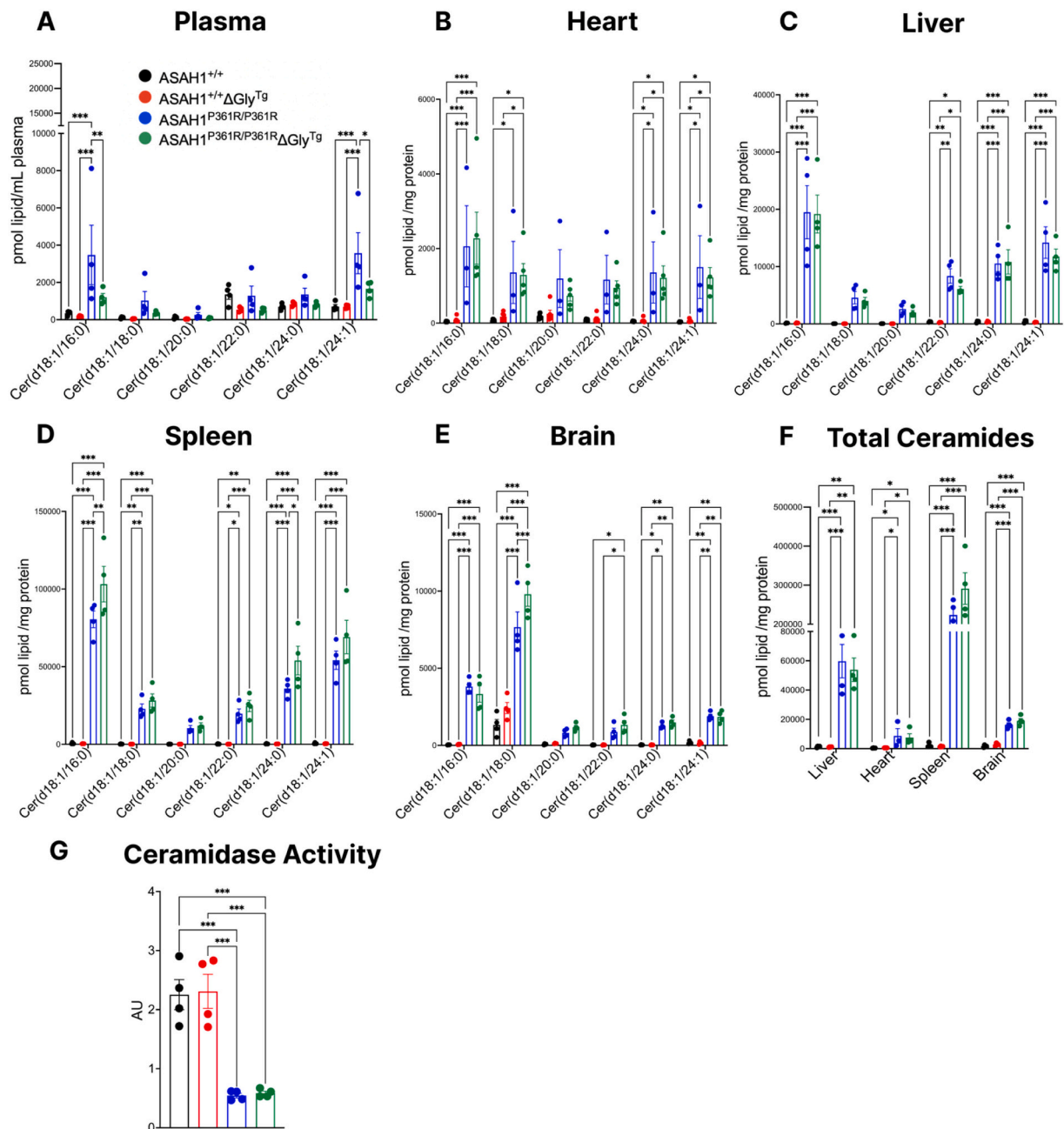

Fig. 3. Adiponectin overexpression lowers ceramides in plasma, but not in tissues of ASAH1$^{P361R/P361R}$ΔGly^{Tg} male mice.
Plasma and tissues from 10-week-old males on a normal chow diet were collected for lipid analysis. (A) Ceramide concentrations in plasma; (B) heart; (C) liver; (D) spleen; (E) brain all analyzed with two-way ANOVAs with multiple comparisons; (F) sum of ceramide species in liver, heart, spleen, and brain analyzed with individual one-way ANOVAs with multiple comparisons. (G) Ceramidase activity assay showing the labeled sphingosine to labeled ceramide ratio in livers of male mice. $n = 4$ per genotype, male mice. Individual values reported with mean ± SEM *$p < 0.05$, **$p < 0.01$, ***$p < 0.001$.
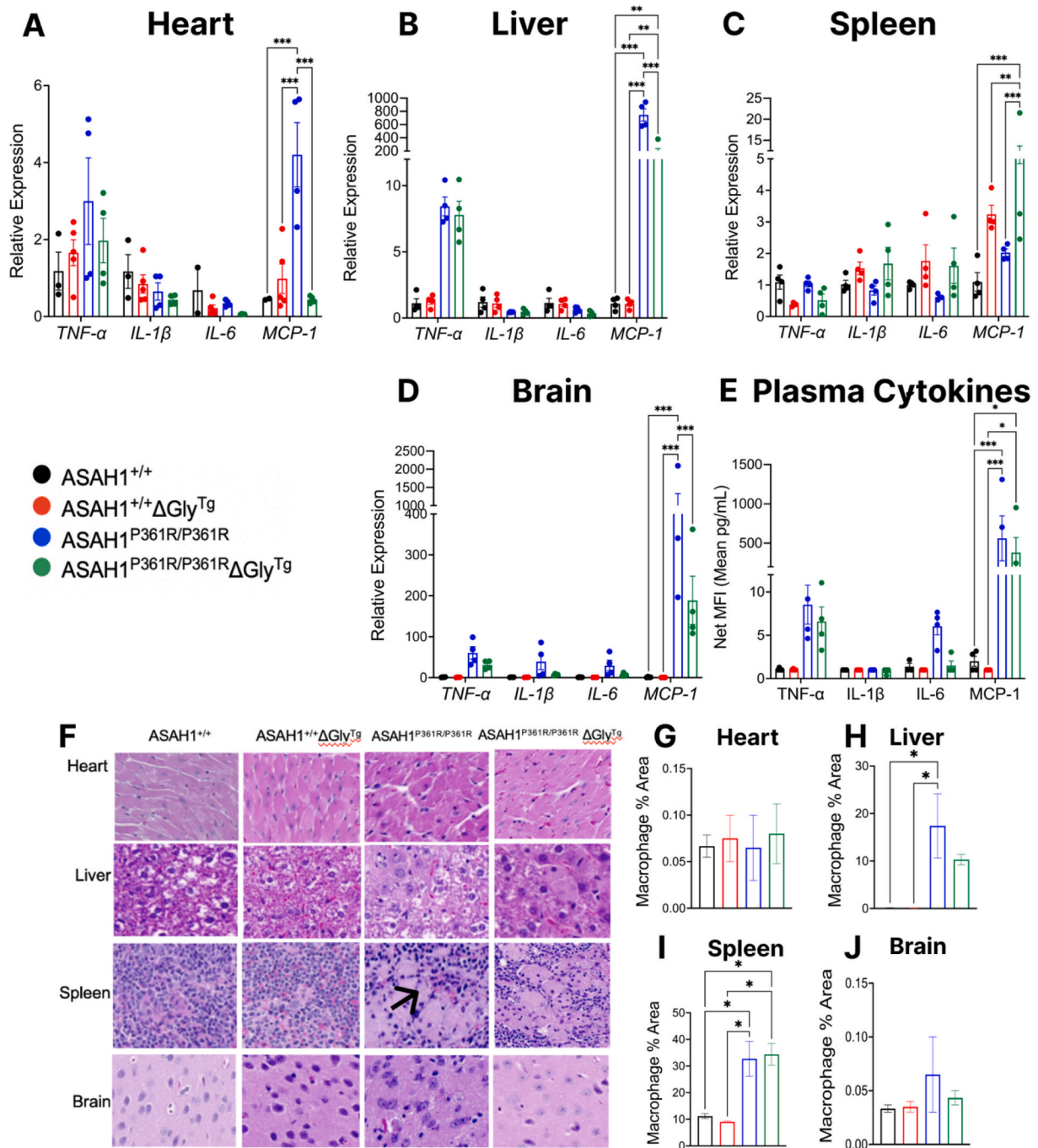
Fig. 4. Adiponectin overexpression in ASAH1$^{P361R/P361R}$ΔGly^{Tg} mice decreases pro-inflammatory cytokines.
Tissues and plasma were harvested 10-week-old males on normal chow diet. Relative mRNA expression of pro-inflammatory cytokines (TNFα, IL-1β, IL-6, and MCP-1) was measured in (A) heart; (B) liver; (C) spleen; and (D) brain ($n = 3$ per genotype), analyzed with two-way ANOVAs with multiple comparisons; (E) Plasma cytokine concentrations ($n = 4$ per genotype); (F) H&E staining of heart, liver, spleen, and brain tissues at 200× zoom (arrow indicates infiltrating macrophages) from male mice; Quantification of infiltrating macrophages in (G) heart; (H) liver; (I) spleen; (J) brain. Individual values reported with mean ± SEM *$p < 0.05$, **$p < 0.01$, ***$p < 0.001$ using male mice.

ASAH1$^{P361R/P361R}$ males, with the most robust reduction observed for MCP-1 in the heart, liver, and brain (Fig. 4A,B,D). Gly adiponectin overexpression did not decrease the expression of pro-inflammatory cytokines in female Farber Disease mice (Appendix D). Surprisingly, adiponectin overexpression increased the expression of pro-inflammatory MCP-1 in the spleens of ASAH1$^{P361R/P361R}$ males (Fig. 4C) and hearts of ASAH1$^{P361R/P361R}$ females (Appendix D). We then measured cytokines in plasma, finding that both male and female Farber Disease mice displayed elevated pro-inflammatory cytokines, especially

MCP-1 (Fig. 4E and Appendix D). Adiponectin overexpression did not significantly reduce plasma pro-inflammatory cytokine concentrations in ASAH1$^{P361R/P361R}$ males or females (Fig. 4E and Appendix D). Finally, histopathologic examination of hematoxylin and eosin (H&E)-stained tissues indicated robust macrophage infiltration in heart, liver, spleen, and brain tissues of Farber Disease mice, which was not reduced with adiponectin overexpression (Fig. 4F-J).

3.5. Adiponectin overexpression improves metabolic abnormalities in heterozygous ASAH1$^{P361R/+}$ mice on a high fat diet

Given the abundance of data implicating both ceramides and adiponectin in the control of glucose and lipid homeostasis, we opted to investigate the heterozygous ASAH1$^{P361R/+}$ mice, which we predicted would be more prone to diet-induced insulin resistance owing to their inability to degrade ceramides. Indeed, male heterozygous ASAH1$^{P361R/+}$ mice displayed increased body mass (Fig. 5B) and a trend towards higher blood glucose (Fig. 5A and Table 1) as compared to wild-type controls. This increased body mass was attributed to significantly increased visceral fat mass, which improved with adiponectin overexpression (Fig. 5C). We did not observe the same pattern in female ASAH1$^{P361R/+}$ mice (Appendix E), which is perhaps unsurprising, given the known resistance of female C57Bl6 mice to gain weight and metabolic disease. After 12 weeks on HFD, we observed no difference in plasma ceramides between ASAH$^{+/+}$ and ASAH1$^{P361R/+}$ males (Fig. 5D).

Given the trends in male body weight and blood glucose, we investigated glucose homeostasis in male mice with a heterozygous Farber Disease mutation (ASAH1$^{P361R/}$). Moreover, we assessed whether ΔGly adiponectin overexpression altered these metabolic responses. Glucose (GTT), insulin (ITT), and pyruvate (PTT) tolerance tests were conducted after 4, 5, and 6 weeks on HFD, respectively, in wild-type and heterozygous ASAH1$^{P361R/+}$ males with and without the ΔGly transgene. Fifteen minutes after glucose injection, ASAH1$^{P361R/+}$ mice had elevated glucose concentrations compared to wild-type ASAH1$^{+/+}$ males, and this trend continued throughout the rest of the GTT (Fig. 5E). Transgenic overexpression of adiponectin normalized glucose concentrations (Fig. 5E,F). Neither the ASAH1 mutations nor adiponectin influenced basal or glucose-stimulated insulin secretion, nor did they influence insulin tolerance (Fig. 5G-I). However, heterozygosity for the P361R ASAH1 mutation increased glucose levels after the pyruvate challenge, suggesting that the animals had increased hepatic glucose production (Fig. 5J,K). Adiponectin overexpression normalized pyruvate-stimulated blood glucose concentrations (Fig. 5J,K).

As these changes in pyruvate tolerance are indicative of alterations in
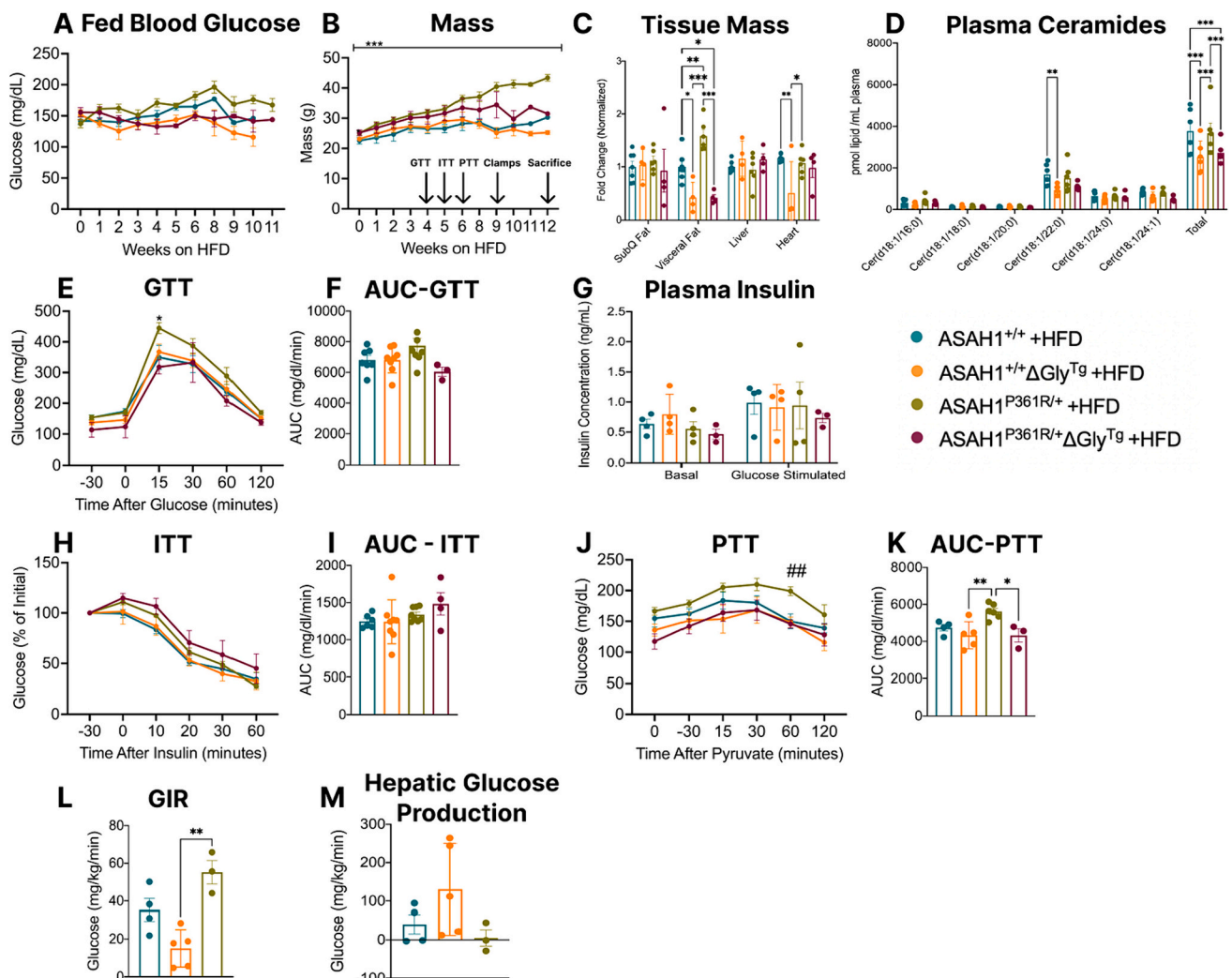

Fig. 5. Metabolic abnormalities observed in heterozygous ASAH1$^{P361R/+}$ males on a high fat diet are improved with adiponectin overexpression.
8-week-old males were placed on a HFD for 12 weeks. (A) blood glucose concentrations during fed state ($n = 8$–10 per genotype); (B) body mass during fed state, *ASAH1$^{+/+}$ versus ASAH1$^{P361R/+}$; (C) Fold change of tissue mass normalized to body weight, $n = 6$ per genotype; (D) plasma ceramide concentrations after 12 weeks on HFD ($n = 4$ per genotype); (E) glucose tolerance after 4 weeks on HFD, $n = 3$–8 per genotype, *ASAH1$^{+/+}$ versus ASAH1$^{P361R/+}$; (F) area under the curve (AUC) for glucose tolerance test; (G) insulin concentrations during glucose tolerance test ($n = 4$ per genotype); (H) insulin tolerance displayed by percent of initial glucose concentration after 5 weeks on HFD ($n = 3$–8 per genotype; (I) AUC insulin tolerance test; (J) pyruvate tolerance after 6 weeks on HFD, #ASAH1$^{P361R/+}$ versus ASAH1$^{P361R/+}$ΔGly^{Tg} ($n = 3$–8 per genotype; (K) AUC pyruvate tolerance test; (L) glucose infusion rate (GIR) and (M) hepatic glucose production during hyperinsulinemic-euglycemic clamps after 9 weeks on HFD ($n = 3$–5 per genotype). Individual values reported with mean ± SEM *$p < 0.05$, **$p < 0.01$, ***$p < 0.001$.

Table 1

Hyperinsulinemic-euglycemic clamps.

	Basal Blood Glucose (mg/dL)	Clamp Blood Glucose (mg/dL)	Glucose Infusion Rate (mg/kg/min)	Glucose Disposal (mg/kg/min)	% Suppression of Glucose production
ASAH1$^{+/+}$ + HFD	148.5 ± 9.6	148.1 ± 5.9	18.3 ± 2.6	23.6 ± 4.0 *	74.3 ± 15.6
ASAH$^{P361R/+}$ + HFD	168.4 ± 9.7	142.5 ± 4.9	7.5 ± 2.0 *	15.6 ± 4.8	43.7 ± 20.2
ASAH1$^{P361R/+}$ΔGly^{Tg} + HFD	103.3 ± 6.9 #	143.7 ± 5.8	18.2 ± 5.1 #	12.8 ± 2.5	103.3 ± 5.1 #

Fasted mice received a continuous infusion of insulin (5 mU/kg/min). Blood glucose levels were measured at 5-minute intervals and maintained at euglycemia by a variable infusion rate of dextrose (30%) mixed with [U-13C]glucose (~50 μmoles/ml). *ASAH1$^{+/+}$ versus ASAH1$^{P361R/+}$; #ASAH1$^{P361R/+}$ versus ASAH1$^{P361R/+}$ΔGly^{Tg}, n=3-5 per genotype. Values reported with mean +/- SEM */#p<0.05.

hepatic insulin sensitivity, we performed hyperinsulinemic-euglycemic clamps after 9 weeks on HFD (Table 1). Euglycemia during the clamp was achieved by targeting the fasting glucose of our wildtype mice (~145 mg/dl), and was not different between genotypes (Table 1). Euglycemic clamp assessments revealed that ASAH1$^{P361R/+}$ males had reduced insulin action evidenced by the decreased glucose infusion rate (GIR) needed to maintain euglycemia (Table 1). Adiponectin overexpression in the ASAH1$^{P361R/+}$ΔGly^{Tg} males markedly improved insulin action evidenced by the increased GIR (Table 1). Whole-body glucose disposal was not improved by adiponectin overexpression. The elevation in GIR observed in ASAH1$^{P361R/+}$ΔGly^{Tg} males was attributed to enhanced suppression of hepatic glucose production, further indicating that adiponectin overexpression improves hepatic insulin resistance.

4. Discussion

Farber Disease is a debilitating and lethal childhood disease caused by acid ceramidase deficiency that currently does not have any approved treatments except for symptom management. The pleiotropic actions of adiponectin have been linked to the intrinsic ceramidase activity of both AdipoR1 and AdipoR2 [33]. Moreover, adiponectin overexpression in mice improves ceramide-dependent lipotoxicity [33,69]. Given the ability of AdipoR1 and AdipoR2 to degrade ceramides when bound to adiponectin, we hypothesized that adiponectin overexpression would lower ceramides and improve outcomes in a mouse model of Farber Disease. We were encouraged by our findings that adiponectin or adiponectin receptor agonist treatments lowered total ceramide content in fibroblasts from a patient with Farber Disease. These findings support previous studies that showed adiponectin enhances acid ceramidase activity in an AdipoR1 and AdipoR2-dependent manner [70–72]. In alignment with the original generation and characterization paper [61], we observed significant elevations of mainly MCP-1 over other cytokines in the Farber Disease mice. We postulate that ceramides drive the release of MCP-1 specifically, which recruits macrophages to aid in ceramide disposal but are unable to degrade ceramide and result in more ceramide storage – leading to their foamy appearance characteristic of Farber Disease. Adiponectin overexpression reduced the expression of pro-inflammatory MCP-1 in the heart, liver, and brain of male Farber Disease mice but not in plasma. We speculate that this male-specific phenomenon may be attributed to the differences in immune cell populations between sexes. Ultimately, adiponectin overexpression did not lower ceramides or improve the severe and immediately life-threatening outcomes in mice modeling Farber Disease. Furthermore, in vivo, adiponectin overexpression did not improve hypoglycemia, growth, tissue macrophage infiltration, or survival in

Farber Disease mice. Finally, treating mice with myriocin, the ceramide synthesis inhibitor, did not increase the lifespan in Farber Disease mice. We postulate that our ΔGly adiponectin overexpression model failed to ameliorate the Farber Disease phenotype because the enhanced utilization of neutral ligand-gated ceramidase was insufficient to compensate for the loss of lysosomal acid ceramidase in multiple tissues.

In addition to investigating adiponectin action in homozygous Farber Disease mice, we explored its effects in mice heterozygous for the Farber Disease mutation when challenged with a high fat diet. As Farber Disease is inherited autosomal recessively, these heterozygous mice model carriers of the Farber Disease mutation including parents and relatives of patients with the disease. Our findings align with our previous study that showed *Asah1* knockout in a murine model was sufficient to induce many features of metabolic syndrome including obesity as well as impaired glucose and lipid metabolism [73]. Knowing that adiponectin is known for its insulin-sensitizing action [59], we were hopeful that adiponectin overexpression would ameliorate outcomes observed on a high-fat diet in heterozygous Farber Disease mice. On a high fat diet, these heterozygous Farber Disease mice demonstrate increased weight gain and hyperglycemia compared to their wild-type controls, which normalize with adiponectin overexpression. This phenomenon was specific to male mice, which typically gain weight on high-fat diets more pronouncedly than female littermates. We speculate that the increased visceral fat mass observed in heterozygous Farber Disease males may be due to an inability to store excess lipids in adipose tissue appropriately. As observed during the PTT, these heterozygous mice have enhanced hepatic glucose production which is blunted by adiponectin overexpression. Finally, hyperinsulinemic-euglycemic clamp assessments confirmed that heterozygous Farber Disease mice had reduced insulin action in the liver, which improved with adiponectin overexpression. With 100 cases of Farber Disease documented, there are a greater number of carriers living worldwide. Based on our studies, these carriers may be at a greater risk for diabetes when stressed by a high-caloric diet.

Ultimately, we hope this study contributes to the Farber Disease literature, guides future Farber Disease studies, and sheds light on potential therapeutics for these patients. Thus far, recombinant human acid ceramidase (ACG-801; Aceragen) remains the most promising treatment for Farber Disease showing improved survival, reduced tissue ceramides, normalized spleen size, reduced plasma levels of MCP-1, and reduced infiltration of macrophages into the liver and spleen in mice modeling Farber Disease during preclinical studies [9]. While not yet FDA-approved, ACG-801 has been granted Rare Pediatric Disease and Fast Track designations by the FDA [74].

5. Conclusion

Our findings indicate that additional strategies are required to ameliorate outcomes of Farber Disease and that carriers of the Farber Disease mutation may be more metabolically vulnerable than non-carriers when stressed by overnutrition.

Declaration of competing interest

None.

Data availability

Data will be made available on request.

Appendix A
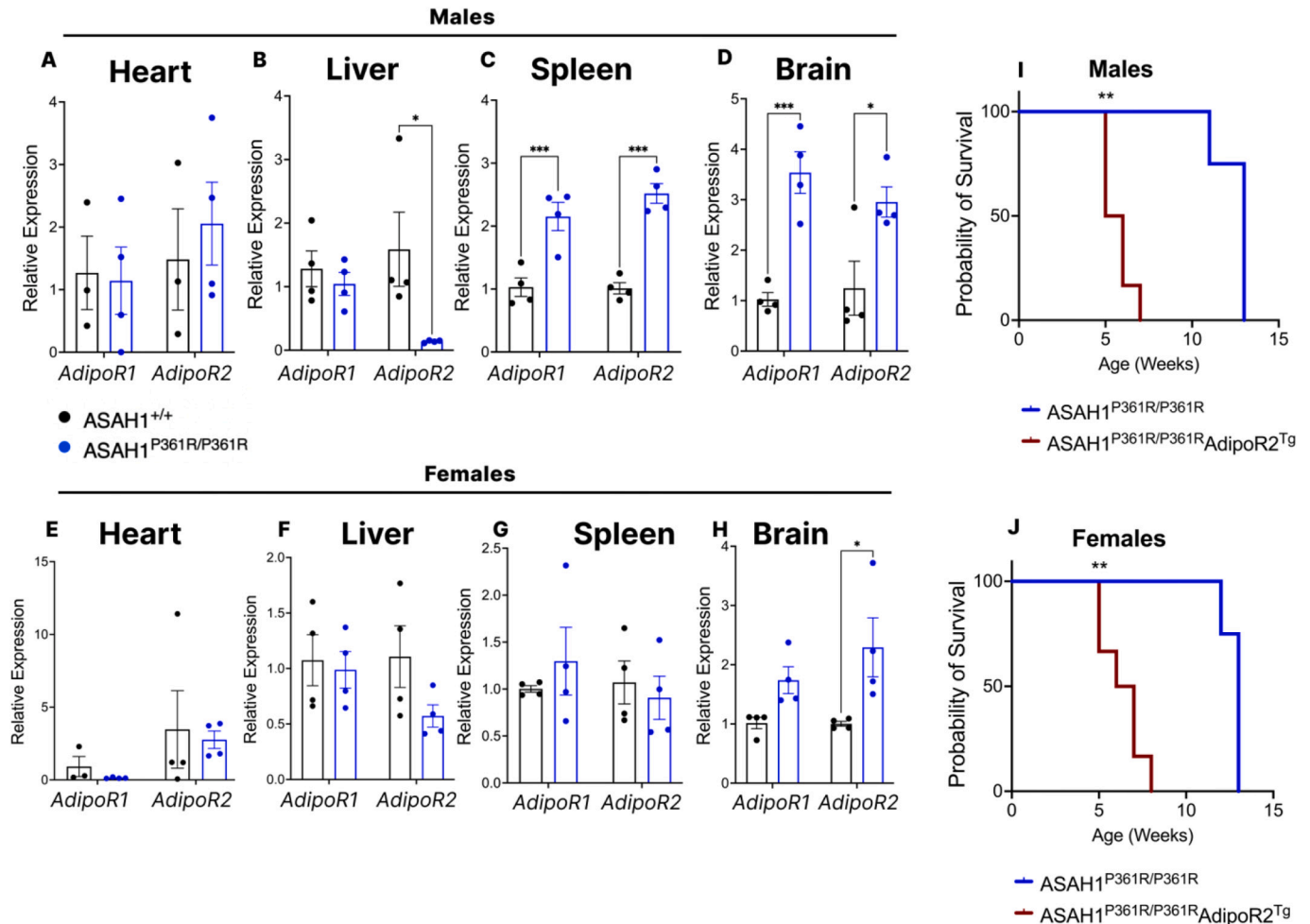
Tissues were harvested 10-week-old males and females on normal chow diet. Relative mRNA expression of *AdipoR1* and *AdipoR2* measured in (A) heart; (B) liver; (C) spleen; and (D) brain from male mice ($n = 4$ per genotype), analyzed with two-way ANOVAs with multiple comparisons; Relative mRNA expression of *AdipoR1* and *AdipoR2* measured in (E) heart; (F) liver; (G) spleen; and (H) brain from female mice ($n = 4$ per genotype), analyzed with two-way ANOVAs with multiple comparisons; (I) Kaplan-Meier survival analysis of male ASAH1[P361R/P361R] mice with and without AdipoR2 overexpression; $n = 4$–6 for each genotype; (J) Kaplan-Meier survival analysis of female ASAH1[P361R/P361R] mice with and without AdipoR2 overexpression; n = 4–6 for each genotype. Individual values reported with mean $\pm$ SEM *$p < 0.05$, **$p < 0.01$, ***$p < 0.001$.

Appendix B
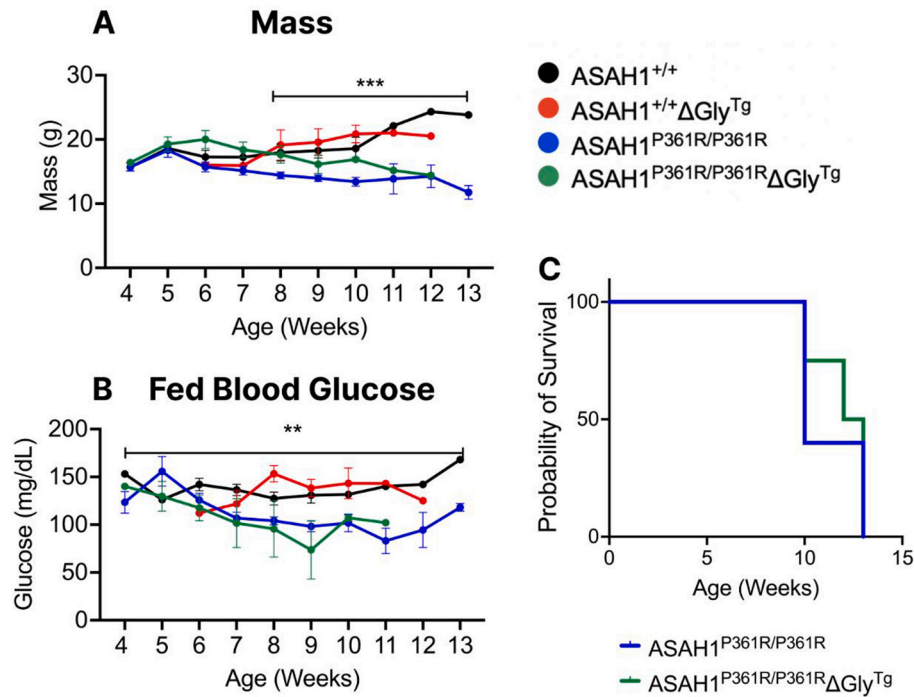
(A) Growth curves of female mice measured in weights versus age; (B) Fed blood glucose curve of female mice; (C) Kaplan-Meier survival analysis of female mice with and without adiponectin overexpression; n = 4–10 for each genotype, female mice. *ASAH1$^{+/+}$ versus ASAH1$^{P361R/P361R}$. Individual values reported with mean ± SEM *p < 0.05, **p < 0.01, ***p < 0.001.

Appendix C
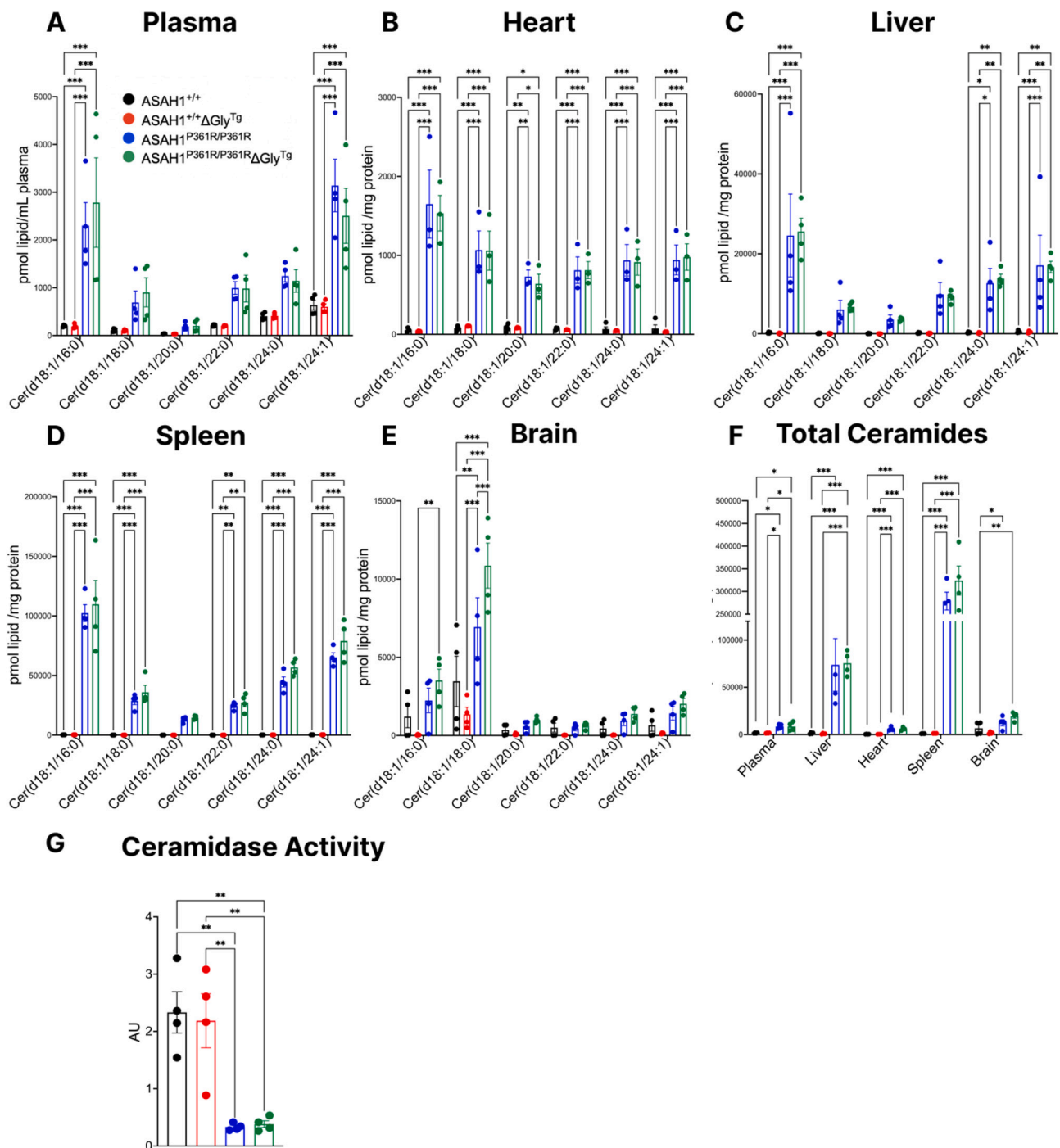
Plasma and tissues from 10-week-old females on a normal chow diet were collected for lipidomics. (A) Ceramide concentrations in plasma; (B) heart; (C) liver; (D) spleen; (E) brain all analyzed with two-way ANOVAs with multiple comparisons; (F) sum of ceramide species in liver, heart, spleen, and brain analyzed with individual one-way ANOVAs with multiple comparisons. (G) Ceramidase activity assay showing the labeled sphingosine to labeled ceramide ratio in livers of female mice. $n = 3$–4 per genotype, female mice. Individual values reported with mean $\pm$ SEM *$p < 0.05$, **$p < 0.01$, ***$p < 0.001$.

Appendix D
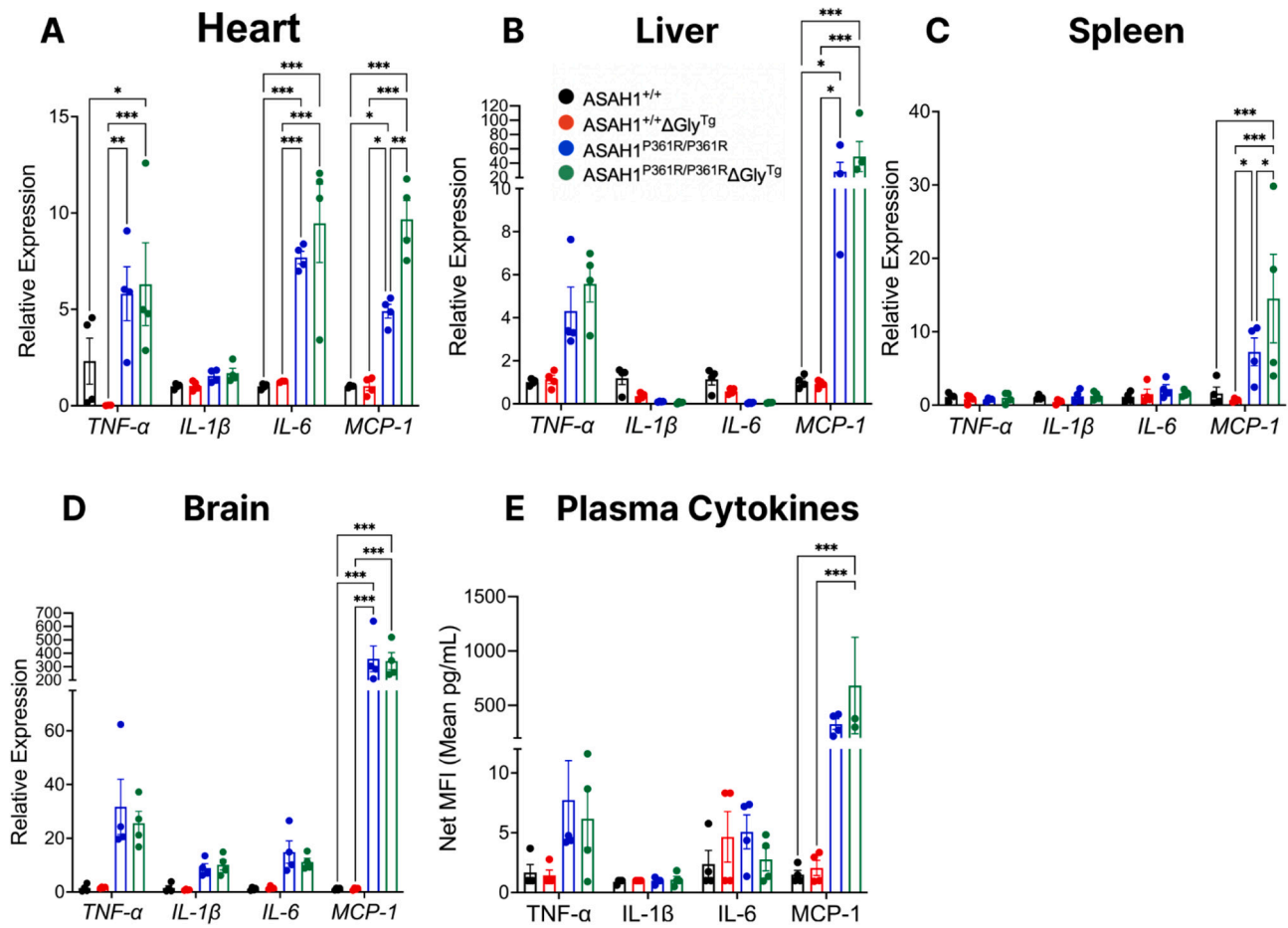
Tissues and plasma were harvested 10-week-old females on normal chow diet. Relative mRNA expression of pro-inflammatory cytokines (*TNFα, IL-1β, IL-6, and MCP-1*) was measured in (A) heart; (B) liver; (C) spleen; and (D) brain (n = 3 per genotype); (E) Plasma cytokine concentrations (n = 4 per genotype); Analyzed with two-way ANOVAs with multiple comparisons; Individual values reported with mean ± SEM *p < 0.05, **p < 0.01, ***p < 0.001 using female mice.

Appendix E
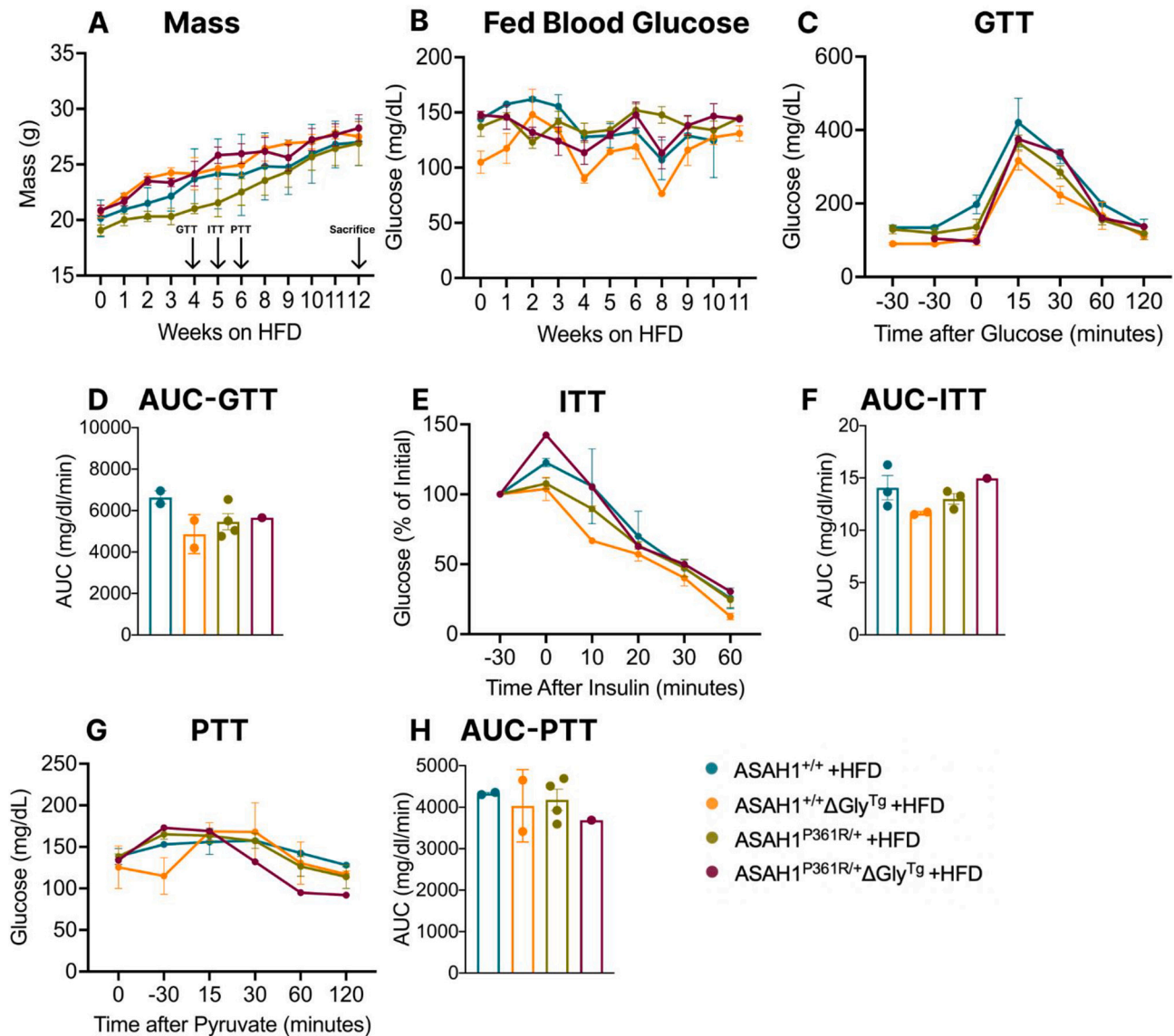
(A) body mass of females during fed state; (B) Fed blood glucose of female mice; (C) glucose tolerance in female mice after 4 weeks on HFD; (D) area under the curve (AUC) for glucose tolerance test; (E) insulin concentrations during glucose tolerance test; (F) insulin tolerance displayed by percent of initial glucose concentration after 5 weeks on HFD in female mice; (F) AUC insulin tolerance test; (G) pyruvate tolerance in female mice after 6 weeks on HFD; (H) AUC pyruvate tolerance test. ($n = 1$–4 per genotype). Individual values reported with mean ± SEM *$p < 0.05$, **$p < 0.01$, ***$p < 0.001$.

References

[1] S. Farber, A lipid metabolic disorder: disseminated lipogranulomatosis; a syndrome with similarity to, and important difference from, Niemann-pick and hand-Schuller-Christian disease, A.M.A. Am. J. Dis. Child. 84 (4) (1952) 499–500. Oct.

[2] Z. Zhang, A.K. Mandal, A. Mital, et al., Human acid ceramidase gene: novel mutations in Farber disease, Mol. Genet. Metab. 70 (4) (2000) 301–309, https://doi.org/10.1006/mgme.2000.3029. Aug.

[3] C. Cozma, M.I. Iurașcu, S. Eichler, et al., C26-ceramide as highly sensitive biomarker for the diagnosis of Farber disease, Sci. Rep. 7 (1) (2017) 6149, https://doi.org/10.1038/s41598-017-06604-2. Jul 21.

[4] M. Torcoletti, A. Petaccia, R.M. Pinto, et al., Farber disease in infancy resembling juvenile idiopathic arthritis: identification of two new mutations and a good early response to allogeneic haematopoietic stem cell transplantation, Rheumatology (Oxford) 53 (8) (2014) 1533–1534, https://doi.org/10.1093/rheumatology/keu010. Aug.

[5] F.P.S. Yu, S. Amintas, T. Levade, J.A. Medin, Acid ceramidase deficiency: Farber disease and SMA-PME, Orphanet J. Rare Dis. 13 (1) (2018) 121, https://doi.org/10.1186/s13023-018-0845-z. Jul 20.

[6] J. Zhou, M. Tawk, F.D. Tiziano, et al., Spinal muscular atrophy associated with progressive myoclonic epilepsy is caused by mutations in ASAH1, Am. J. Hum. Genet. 91 (1) (2012) 5–14, https://doi.org/10.1016/j.ajhg.2012.05.001. Jul 13.

[7] M.S. Nagree, J. Rybova, A. Kleynerman, et al., Spinal muscular atrophy-like phenotype in a mouse model of acid ceramidase deficiency, Commun. Biol. 6 (1) (2023) 560, https://doi.org/10.1038/s42003-023-04932-w. May 25.

[8] E.H. Schuchman, Acid ceramidase and the treatment of ceramide diseases: the expanding role of enzyme replacement therapy, Biochim. Biophys. Acta 1862 (9) (2016) 1459–1471, https://doi.org/10.1016/j.bbadis.2016.05.001. Sep.

[9] X. He, S. Dworski, C. Zhu, et al., Enzyme replacement therapy for Farber disease: proof-of-concept studies in cells and mice, BBA Clin. 7 (2017) 85–96, https://doi.org/10.1016/j.bbacli.2017.02.001. Jun.

[10] NORD, ASAH1-Related Disorders. https://rarediseases.org/rare-diseases/farbers-disease/. (Accessed 7 September 2020).

[11] S.A. Summers, B. Chaurasia, W.L. Holland, Metabolic messengers: ceramides, Nat. Metab. 1 (11) (2019) 1051–1058, https://doi.org/10.1038/s42255-019-0134-8. Nov.

[12] H.L. Brockman, M.M. Momsen, R.E. Brown, et al., The 4,5-double bond of ceramide regulates its dipole potential, elastic properties, and packing behavior, Biophys. J. 87 (3) (2004) 1722–1731, https://doi.org/10.1529/biophysj.104.044529. Sep.

[13] B. Chaurasia, T.S. Tippetts, R. Mayoral Monibas, et al., Targeting a ceramide double bond improves insulin resistance and hepatic steatosis, Science. 365 (6451) (2019) 386–392, https://doi.org/10.1126/science.aav3722. Jul 26.

[14] S.A. Summers, Ceramides: nutrient signals that drive Hepatosteatosis, J. Lipid Atheroscler. 9 (1) (2020) 50–65, https://doi.org/10.12997/jla.2020.9.1.50. Jan.

[15] B. Chaurasia, S.A. Summers, Ceramides - Lipotoxic inducers of metabolic disorders, Trends Endocrinol. Metab. 26 (10) (2015) 538–550, https://doi.org/10.1016/j.tem.2015.07.006. Oct.

[16] S.A. Summers, Could ceramides become the new cholesterol? Cell Metab. 27 (2) (2018) 276–280, https://doi.org/10.1016/j.cmet.2017.12.003. Feb 6.

[17] W.L. Holland, S.A. Summers, Sphingolipids, insulin resistance, and metabolic disease: new insights from in vivo manipulation of sphingolipid metabolism, Endocr. Rev. 29 (4) (2008) 381–402. Jun.

[18] W.L. Holland, J.T. Brozinick, L.P. Wang, et al., Inhibition of ceramide synthesis ameliorates glucocorticoid-, saturated-fat-, and obesity-induced insulin resistance, Cell Metab. 5 (3) (2007) 167–179, https://doi.org/10.1016/j.cmet.2007.01.002. Mar.

[19] B.T. Bikman, Y. Guan, G. Shui, et al., Fenretinide prevents lipid-induced insulin resistance by blocking ceramide biosynthesis, J. Biol. Chem. 287 (21) (2012) 17426–17437, https://doi.org/10.1074/jbc.M112.359950. May 18.

[20] J.R. Ussher, T.R. Koves, V.J. Cadete, et al., Inhibition of de novo ceramide synthesis reverses diet-induced insulin resistance and enhances whole-body oxygen consumption, Diabetes. 59 (10) (2010) 2453–2464, https://doi.org/10.2337/db09-1293. Oct.

[21] M.R. Hojjati, Z. Li, H. Zhou, et al., Effect of myriocin on plasma sphingolipid metabolism and atherosclerosis in apoE-deficient mice, J Biol Chem. 280 (11) (2005) 10284–10289. Mar 18.

[22] M.R. Hojjati, Z. Li, X.C. Jiang, Serine palmitoyl-CoA transferase (SPT) deficiency and sphingolipid levels in mice, Biochim. Biophys. Acta 1737 (1) (2005) 44–51. Oct 15.

[23] X.C. Jiang, I.J. Goldberg, T.S. Park, Sphingolipids and cardiovascular diseases: lipoprotein metabolism, atherosclerosis and cardiomyopathy, Adv. Exp. Med. Biol. 721 (2011) 19–39, https://doi.org/10.1007/978-1-4614-0650-1_2.

[24] T.S. Park, W. Rosebury, E.K. Kindt, M.C. Kowala, R.L. Panek, Serine palmitoyltransferase inhibitor myriocin induces the regression of atherosclerotic plaques in hyperlipidemic ApoE-deficient mice, Pharmacol. Res. 58 (1) (2008) 45–51, https://doi.org/10.1016/j.phrs.2008.06.005. Jul.

[25] S.B. Russo, C.F. Baicu, A. Van Laer, et al., Ceramide synthase 5 mediates lipid-induced autophagy and hypertrophy in cardiomyocytes, J. Clin. Invest. 122 (11) (2012) 3919–3930, https://doi.org/10.1172/JCI63888. Nov.

[26] G. Yang, L. Badeanlou, J. Bielawski, A.J. Roberts, Y.A. Hannun, F. Samad, Central role of ceramide biosynthesis in body weight regulation, energy metabolism, and the metabolic syndrome, Am. J. Physiol. Endocrinol. Metab. 297 (1) (2009) E211–E224, https://doi.org/10.1152/ajpendo.91014.2008. Jul.

[27] T.S. Park, Y. Hu, H.L. Noh, et al., Ceramide is a cardiotoxin in lipotoxic cardiomyopathy, J. Lipid Res. 49 (10) (2008) 2101–2112, https://doi.org/10.1194/jlr.M800147-JLR200. Oct.

[28] J.B. Polya, R.S. Parsons, Free ceramide in blood and its relevance to atherosclerosis. I, Med. J. Aust. 1 (18) (1973) 873–879. May 5.

[29] J. Bismuth, P. Lin, Q. Yao, C. Chen, Ceramide: a common pathway for atherosclerosis? Atherosclerosis. 196 (2) (2008) 497–504, https://doi.org/10.1016/j.atherosclerosis.2007.09.018. Feb.

[30] S.A. Summers, Ceramides in insulin resistance and lipotoxicity, Prog. Lipid Res. 45 (1) (2006) 42–72. Jan.

[31] M. Kolak, J. Gertow, J. Westerbacka, et al., Expression of ceramide-metabolising enzymes in subcutaneous and intra-abdominal human adipose tissue, Lipids Health Dis. 11 (2012) 115, https://doi.org/10.1186/1476-511X-11-115. Sep 13.

[32] J.A. Chavez, S.A. Summers, A ceramide-centric view of insulin resistance, Cell Metab. 15 (5) (2012) 585–594, https://doi.org/10.1016/j.cmet.2012.04.002. May 2.

[33] W.L. Holland, R.A. Miller, Z.V. Wang, et al., Receptor-mediated activation of ceramidase activity initiates the pleiotropic actions of adiponectin, Nat. Med. 17 (1) (2011) 55–63, https://doi.org/10.1038/nm.2277. Jan.

[34] W.L. Holland, B.T. Bikman, L.P. Wang, et al., Lipid-induced insulin resistance mediated by the proinflammatory receptor TLR4 requires saturated fatty acid-induced ceramide biosynthesis in mice, J. Clin. Invest. 121 (5) (2011) 1858–1870. May 2. (doi:43378 pii. 10.1172/JCI43378).

[35] B.T. Bikman, S.A. Summers, Ceramides as modulators of cellular and whole-body metabolism, J. Clin. Invest. 121 (11) (2011) 4222–4230, https://doi.org/10.1172/JCI57144. Nov.

[36] B.T. Bikman, S.A. Summers, Sphingolipids and hepatic steatosis, Adv. Exp. Med. Biol. 721 (2011) 87–97, https://doi.org/10.1007/978-1-4614-0650-1_6.

[37] S.A. Summers, Sphingolipids and insulin resistance: the five Ws, Curr. Opin. Lipidol. 21 (2) (2010) 128–135, https://doi.org/10.1097/MOL.0b013e3283373b66. Apr.

[38] W.L. Holland, T.A. Knotts, J.A. Chavez, L.P. Wang, K.L. Hoehn, S.A. Summers, Lipid mediators of insulin resistance, Nutr. Rev. 65 (6 Pt 2) (2007) S39–S46. Jun.

[39] S.A. Summers, D.H. Nelson, A role for sphingolipids in producing the common features of type 2 diabetes, metabolic syndrome X, and Cushing's syndrome, Diabetes. 54 (3) (2005) 591–602. Mar.

[40] Q.J. Zhang, W.L. Holland, L. Wilson, et al., Ceramide mediates vascular dysfunction in diet-induced obesity by PP2A-mediated dephosphorylation of the eNOS-Akt complex, Diabetes. 61 (7) (2012) 1848–1859, https://doi.org/10.2337/db11-1399. Jul.

[41] T.S. Park, R.L. Panek, M.D. Rekhter, et al., Modulation of lipoprotein metabolism by inhibition of sphingomyelin synthesis in ApoE knockout mice, Atherosclerosis. 189 (2) (2006) 264–272. Dec.

[42] T.S. Park, I.J. Goldberg, Sphingolipids, lipotoxic cardiomyopathy, and cardiac failure, Heart Fail. Clin. 8 (4) (2012) 633–641, https://doi.org/10.1016/j.hfc.2012.06.003. Oct.

[43] S.Y. Lee, J.R. Kim, Y. Hu, et al., Cardiomyocyte specific deficiency of serine palmitoyltransferase subunit 2 reduces ceramide but leads to cardiac dysfunction, J. Biol. Chem. 287 (22) (2012) 18429–18439, https://doi.org/10.1074/jbc.M111.296947. May 25.

[44] R. Ji, H. Akashi, K. Drosatos, et al., Increased de novo ceramide synthesis and accumulation in failing myocardium, JCI Insight. 2 (9) (2017), https://doi.org/10.1172/jci.insight.82922. May 4.

[45] B. Westra, Ceramides, Plasma [A Test in Focus]. Mayo Clinic, Mayo Medical Laboratories, Accessed February 23, 2017, https://news.mayomedicallaboratories.com/2016/07/28/ceramides-plasma-a-test-in-focus/, 2017.

[46] R. Laaksonen, K. Ekroos, M. Sysi-Aho, et al., Plasma ceramides predict cardiovascular death in patients with stable coronary artery disease and acute coronary syndromes beyond LDL-cholesterol, Eur. Heart J. 37 (25) (2016) 1967–1976, https://doi.org/10.1093/eurheartj/ehw148. Jul 1.

[47] J.M. Cheng, M. Suoniemi, I. Kardys, et al., Plasma concentrations of molecular lipid species in relation to coronary plaque characteristics and cardiovascular outcome: results of the ATHEROREMO-IVUS study, Atherosclerosis. 243 (2) (2015) 560–566, https://doi.org/10.1016/j.atherosclerosis.2015.10.022. Dec.

[48] K. Tarasov, K. Ekroos, M. Suoniemi, et al., Molecular lipids identify cardiovascular risk and are efficiently lowered by simvastatin and PCSK9 deficiency, J. Clin. Endocrinol. Metab. 99 (1) (2014) E45–E52, https://doi.org/10.1210/jc.2013-2559. Jan.

[49] J. Yu, W. Pan, R. Shi, et al., Ceramide is upregulated and associated with mortality in patients with chronic heart failure, Can. J. Cardiol. 31 (3) (2015) 357–363, https://doi.org/10.1016/j.cjca.2014.12.007. Mar.

[50] W. Pan, J. Yu, R. Shi, et al., Elevation of ceramide and activation of secretory acid sphingomyelinase in patients with acute coronary syndromes, Coron. Artery Dis. 25 (3) (2014) 230–235, https://doi.org/10.1097/MCA.0000000000000079. May.

[51] A.S. Havulinna, M. Sysi-Aho, M. Hilvo, et al., Circulating ceramides predict cardiovascular outcomes in the population-based FINRISK 2002 cohort, Arterioscler. Thromb. Vasc. Biol. 36 (12) (2016) 2424–2430, https://doi.org/10.1161/ATVBAHA.116.307497. Dec.

[52] B.C. Bergman, J.T. Brozinick, A. Strauss, et al., Serum sphingolipids: relationships to insulin sensitivity and changes with exercise in humans, Am. J. Physiol. Endocrinol. Metab. 309 (4) (2015) E398–E408, https://doi.org/10.1152/ajpendo.00134.2015. Aug 15.

[53] J.M. Haus, S.R. Kashyap, T. Kasumov, et al., Plasma ceramides are elevated in obese subjects with type 2 diabetes and correlate with the severity of insulin resistance, Diabetes. 58 (2) (2009) 337–343, https://doi.org/10.2337/db08-1228. Feb.

[54] J. Boon, A.J. Hoy, R. Stark, et al., Ceramides contained in LDL are elevated in type 2 diabetes and promote inflammation and skeletal muscle insulin resistance, Diabetes. 62 (2) (2013) 401–410, https://doi.org/10.2337/db12-0686. Feb.

[55] X. Lopez, A.B. Goldfine, W.L. Holland, R. Gordillo, P.E. Scherer, Plasma ceramides are elevated in female children and adolescents with type 2 diabetes, J. Pediatr. Endocrinol. Metab. 26 (9–10) (2013) 995–998, https://doi.org/10.1515/jpem-2012-0407.

[56] V.D. de Mello, M. Lankinen, U. Schwab, et al., Link between plasma ceramides, inflammation and insulin resistance: association with serum IL-6 concentration in patients with coronary heart disease, Diabetologia. 52 (12) (2009) 2612–2615, https://doi.org/10.1007/s00125-009-1482-9. Dec.

[57] S.A. Summers, Could ceramides become the new cholesterol? Cell Metab. (2017) https://doi.org/10.1016/j.cmet.2017.12.003. Dec 26.

[58] Clinic M, MI Heart ceramides, in: Mayo Clinic Laboratories, 2022. Accessed 12/16/2022, https://news.mayocliniclabs.com/ceramides-miheart/.

[59] J.A.M. Mala Sharma, Nader G. Abraham, Adiponectin: A mediator of obesity, insulin resistance, diabetes, and the metabolic syndrome, in: McClung WSAaJA (Ed.), Translational Research in Coronary Artery Disease: Pathophysiology to Treatment, Elsevier Science & Technology, 2016.

[60] T. Yamauchi, Y. Nio, T. Maki, et al., Targeted disruption of AdipoR1 and AdipoR2 causes abrogation of adiponectin binding and metabolic actions, Nat. Med. 13 (3) (2007) 332–339, https://doi.org/10.1038/nm1557. Mar.

[61] A.M. Alayoubi, J.C. Wang, B.C. Au, et al., Systemic ceramide accumulation leads to severe and varied pathological consequences, EMBO Mol. Med. 5 (6) (2013) 827–842, https://doi.org/10.1002/emmm.201202301. Jun.

[62] J. Rybova, L. Kuchar, J. Sikora, W.M. McKillop, J.A. Medin, Skin inflammation and impaired adipogenesis in a mouse model of acid ceramidase deficiency, J. Inherit. Metab. Dis. 45 (6) (2022) 1175–1190, https://doi.org/10.1002/jimd.12552. Nov.

[63] T.P. Combs, U.B. Pajvani, A.H. Berg, et al., A transgenic mouse with a deletion in the collagenous domain of adiponectin displays elevated circulating adiponectin and improved insulin sensitivity, Endocrinology. 145 (1) (2004) 367–383, https://doi.org/10.1210/en.2003-1068. Jan.

[64] J.A. Medin, T. Takenaka, S. Carpentier, et al., Retrovirus-mediated correction of the metabolic defect in cultured Farber disease cells, Hum. Gene Ther. 10 (8) (1999) 1321–1329, https://doi.org/10.1089/10430349950018003. May 20.

[65] T. Levade, H.W. Moser, A.H. Fensom, K. Harzer, A.B. Moser, R. Salvayre, Neurodegenerative course in ceramidase deficiency (Farber disease) correlates with the residual lysosomal ceramide turnover in cultured living patient cells, J. Neurol. Sci. 134 (1–2) (1995) 108–114, https://doi.org/10.1016/0022-510x(95)00231-0. Dec.

[66] W.L. Holland, J.Y. Xia, J.A. Johnson, et al., Inducible overexpression of adiponectin receptors highlight the roles of adiponectin-induced ceramidase signaling in lipid and glucose homeostasis, Mol. Metab. 6 (3) (2017) 267–275, https://doi.org/10.1016/j.molmet.2017.01.002. Mar.

[67] V. Matyash, G. Liebisch, T.V. Kurzchalia, A. Shevchenko, D. Schwudke, Lipid extraction by methyl-tert-butyl ether for high-throughput lipidomics, J. Lipid Res. 49 (5) (2008) 1137–1146, https://doi.org/10.1194/jlr.D700041-JLR200. May.

[68] C. Mao, R. Xu, Z.M. Szulc, A. Bielawska, S.H. Galadari, L.M. Obeid, Cloning and characterization of a novel human alkaline ceramidase. A mammalian enzyme that hydrolyzes phytoceramide, J. Biol. Chem. 276 (28) (2001) 26577–26588, https://doi.org/10.1074/jbc.M102818200. Jul 13.

[69] S.A. Summers, The ART of lowering ceramides, Cell Metab. 22 (2) (2015) 195–196, https://doi.org/10.1016/j.cmet.2015.07.019. Aug 4.

[70] G. Li, Q. Zhang, J. Hong, J.K. Ritter, P.L. Li, Inhibition of pannexin-1 channel activity by adiponectin in podocytes: role of acid ceramidase activation, Biochim. Biophys. Acta Mol. Cell Biol. Lipids 1863 (10) (2018) 1246–1256, https://doi.org/10.1016/j.bbalip.2018.07.016. Oct.

[71] Y. Kim, J.H. Lim, E.N. Kim, et al., Adiponectin receptor agonist ameliorates cardiac lipotoxicity via enhancing ceramide metabolism in type 2 diabetic mice, Cell Death Dis. 13 (3) (2022) 282, https://doi.org/10.1038/s41419-022-04726-8. Mar 30.

[72] S.R. Choi, J.H. Lim, M.Y. Kim, et al., Adiponectin receptor agonist AdipoRon decreased ceramide, and lipotoxicity, and ameliorated diabetic nephropathy, Metabolism. 85 (2018) 348–360, https://doi.org/10.1016/j.metabol.2018.02.004. Aug.

[73] B. Chaurasia, L. Ying, C.L. Talbot, et al., Ceramides are necessary and sufficient for diet-induced impairment of thermogenic adipocytes, Mol. Metab. 45 (2021) 101145, https://doi.org/10.1016/j.molmet.2020.101145. Mar.

[74] Sciences R, Enzyvant's Investigational Farber Disease Enzyme Replacement Therapy, RVT-801, Receives FDA Fast Track and Rare Pediatric Disease Designations. https://roivant.com/enzyvant%E2%80%99s-investigational-farber-disease-enzyme-replacement-therapy-rvt-801-receives-fda-fast-track-and-rare-pediatric-disease-designations.html. (Accessed 20 September 2020).